Miscellaneous effects

P. Skensved and B.C. Robertson
SNO-STR-90-28

28-Feb-1990

Introduction

This document deals with number of different things not included in earlier Monte Carlo reports plus topics identified at the LANL meeting such as scattered light and its effect on time fitters, the implications of increased radioactivity in the Acrylic, 'late' tubes and 'black' reflectors.

Effects of scattered light on Time Fitters

Our Monte Carlo code uses a simple time fitter to reconstruct the events. For each tube hit, it evaluates the transit time difference :

$$\Delta t_i = \frac{n}{c}|\vec{r}_i - \vec{r}| - (t_i - t)$$

If one ignores scattering and the finite size of the PMT then Δt_i is the time spread in the PMT and, since we assume it to be gaussian

$$\chi^2 = \frac{1}{n-4}\sum_{i=1}^{n}\left(\frac{\Delta t_i}{\sigma_i}\right)^2$$

has a χ^2 distribution with $n-4$ degrees of freedom which can be minimized using ordinary non-linear least squares techniques. σ_i is the time spread of the PMT. Only a subset of the tubes are presented to the fitter. Various early and late cuts are employed to reduce the number of random noise tubes and tubes which have scattered light. Detail can be found in [1]. In the final fitter pass only tubes for which $|\Delta t_i|$ is less than $2.4 \times \sigma_i$ are included. This sets an upper limit on χ^2 and it also set a limit on how much extra distance scattered light can travel.

Figure 1 shows the distribution of $-\Delta t_i$ for one thousand 3.511 MeV electrons started at the center of the D_2O along the x-axis. Figure 1a shows the total distribution, 1b what happens when noise hits are excluded and finally figure 1c shows what is left when scattered hits are removed as well. We have used the source position and time for $\vec{r}$ and t in this case. Even with a narrow window around the peak it is clear that a certain amount of scattered light will always be included. This broadens the peak a little and adds a tail on the right hand side leading to an increased uncertainty in the fitted position and more importantly to a systematic shift in the average fitted position. The shift is 'forward' - that is in the direction of the event. From the definition of Δt_i it is clear that a time fitter likes to 'straighten out' any delayed photon track in such a way that all the other distances change by the same amount. What is not so clear is why this always results in a net forward movement on the average. The reason for this can be understood by looking at a simple model. Let us for simplicity assume that σ_i is a constant. Then, if $\vec{a} = (x, y, z, t)$ is a point close to the minimum and $\vec{a} + \vec{\delta a}$ is the minimum, we can set up a set of first order equations for $\vec{\delta a}$:

$$\sum_{k=1}^{4} \left\{ \sum_{i=1}^{n} \frac{\partial \Delta t_i}{\partial a_k} \frac{\partial \Delta t_i}{\partial a_j} \right\} \delta a_j = -\sum_{i=1}^{n} \Delta t_i \frac{\partial \Delta t_i}{\partial a_j}$$

which are trivial to solve since the matrix is symmetric. The direction of the drive $\vec{\delta a}$ is determined by the signs of the off-diagonal matrix elements, that is by sums of type $(x_i - x) \times (y_i - y)$.

While this model is exact it is hard to visualize. The effects are best illustrated by a simple picture in 2 dimensions. Figures 2 and 3 shows an 'event' placed in the center with a typical non-isotropic light distribution chosen to look like Čerenkov light from an electron traveling along the x-

axis. The dotted lines represent prompt photons, the dashed line a delayed photon. Figure 4 shows en 'event' near the wall. In both cases the delay is 2 ns. The direction of the drive is indicated by the arrow and the magnitude is written on each figure.

It is seen that late hits beyond a certain critical angle drives the vertex forward. Futhermore, it is clear that for the same delay, a late backward photon will move the vertex more than a forward one. This explains why the average drive is forward and why removing hits in a backward hemisphere will not reduce the drive to zero. It also points out the importance of backward prompt photons in determining the correct vertex.

Maximum effect of 'zero pulling'

To get an idea of what the implications of the pulling by the fitter are, we have reanalyzed data sets created for [2]. Events originating inside the D_2O were fitted and sorted with a radial cut of 650 cm but tabulated as if they reconstructed inside 600. Any event generated outside 600 cm was assumed to reconstruct outside and therefore not included in the table. This gives an overestimate of what the possible improvement is in that it is equivalent to : zero timing resolution, no systematics in the reconstruction, no scattered light and γ's converting in zero distance.

Figures 5 shows the Mark II detector with roughly 30% hard coverage and reflectors with 2.5 ns PMTs from [2]. In figure 6 the same data is reanalyzed is indicated above. It is clear that the effect on the background near the threshold is minimal - about a factor of 2.5 or about 200 keV in threshold. A similar analysis for the case labeled 20g in [2] (2698 twenty inch tubes with 5 ns timing) can be found in figures 7 and 8. The difference here is a little greater - about a factor of 3 (about 300 keV in threshold).

Correcting for the fact that the source of background here is caused mainly by low energy γ's from the decay of Th we can safely conclude that fitter systematics accounts for *less* than a factor of 2 or *less* than 200 keV in threshold. While more fitter development should take place it should not take on undue priority as it will not affect comparisons between different

tube options to any significant degree.

Increased radioactivity in Acrylic

In terms of 'what if' scenarios, the most worrisome is probably the question of increased radioactivity in the Acrylic above what is assumed in SNO-87-12. We have reanalyzed the data in [2] with the assumption that the Acrylic is 10 times more radioactive. Figure 9 shows what happens to the Mark II design (compare with figure 5). There is a shift in threshold of about 600 keV which would not compromise the Charged Current or the Elastic Scattering measurements. For comparison, figure 10 shows the spectrum if the H_2O has Th and U levels 10 times above our assumed values.

The effect on the Neutral Current measurement is much bigger. Using the full D_2O volume is no longer possible as the signal to background ratio deteriorates to about one to one. Radial distributions are plotted in figure 11a (signal, internal background and external background as function of r^3) and in 11b (total as function of r). Both are with an energy cut of 5 MeV. The Acrylic is in channels 22 and 60 (top and bottom figure). Table 2 lists the number of integral counts above E between 3 and 8 MeV for various radial cuts. The first entry is for the standard radioactivity level, the second is for the higher one. From the figures and the table it is clear that we will effectively lose more than half the fiducial volume. At this level we would be back to the original Mark II situation where the determining factor in extracting the NC flux would be how well we could measure the U/Th levels in the D_2O. Determining the neutron-induced background from the Acrylic by looking at the slope of the 'wall' between 4 and 6 MeV (see fig. 9) is not possible since we would have to isolate the Acrylic component and separately determine the Th and U contamination levels. The two isotopes contribute very differently to the CC and NC backgrounds.

A similar analysis with 10 times higher radioactivity was carried out for the 57%, 20" tube case (case 20g in [2]). The results are plotted in figures 12 and 13 and the conclusions are the same as above.

N_{hit}	E(MeV)	r_{fit}<600			r_{fit}<550			r_{fit}<500		
		nc	int	ext	nc	int	ext	nc	int	ext
21	2.93	3515	1132	250	3041	994	117	2453	797	33
				1932			853			257
29	4.04	3348	1071	234	2898	943	106	2345	756	30
				1820			802			257
36	5.02	2841	908	190	2474	804	91	2021	649	25
				1456			628			204
43	6.00	1969	600	120	1730	531	52	1429	427	14
				934			393			130
50	6.97	1001	306	52	890	277	25	745	229	6
				426			170			62
57	7.95	365	120	31	330	107	12	271	94	3
				129			56			28
M.C. Events		3742	1191	3161	3742	1191	316	3742	1191	316
				2433			2433			2433

Table 1: Integral number of Neutral Current events and background events (neutron induced only) reconstructed inside fiducial volume per year assuming standard radioactivity and ten times the activity in the Acrylic.

	1 ns	2 ns	5 ns
1%	32.1 (61.5)	20.8 (50.6)	18.1 (51.1)
5%	34.6 (62.8)	23.4 (53.3)	20.9 (53.7)
10%	39.8 (71.9)	31.0 (61.4)	26.1 (61.3)

Table 2: Longitudinal deviation in cm as function of PMT timing (FWHM) and percentage late hits (10 ns delay). Numbers in brackets are second moments of distribution.

Late tube study

During the phototube testing program at Queen's we have seen that a certain type of PMT sometimes produces pulses which are delayed by approximately 10 ns. In view of what has been said previously about the effects of scattered (ie. late) light it is obvious that such behaviour could be a problem. A Monte Carlo study was consequently done to determine what level of late pulsing can be tolerated. The code was modified to delay a certain fraction of the pulses by 10 ns and the fraction was set to 1%, 5% and 10%. A total of one thousand 6.511 MeV total energy electrons were started randomly in the D_2O into 4π. The model chosen had 6600 twelve inch PMTs giving 50% 'hard' coverage. Different timings were tried; 1.0, 2.5 and 5.0 ns. The respective results are summarized in figures 14, 15 and 16 where the longitudinal component of the reconstruction deviation is histogrammed. The top figure is for 1% late hits, the middle for 5% and the bottom is for 10%. The first and second moments of the distributions are shown in table 2.

A limit of 2% should be set on 'late' pulsing in the PMT specifications. Note that this refers to *correlated* late pulsing rather than *random* late pulsing. The limit on random late pulsing is effectively included in the dark pulse rate used in the simulation (set to 1,000 s^{-1} for the small tubes and 2,000 s^{-1} for the 20" tube).

'Black' Reflectors

Another 'what if' type question is what happens if we use reflectors and they go bad. We have done a set of simulations with approximately 30% 'hard' coverage and 2.5 *ns* timing with 'black' reflectors. This case is similar to the one labeled 8j in [2] and shown in figure 5. Any photon striking one of these 'black' reflectors is assumed to be absorbed immediately. In reality a non-working reflector would probably be gray rather than black and still reflect some light.

The results are presented in figure 17. The number of photons collected per MeV electron energy is reduced by a factor of 2 and the energy resolution suffers greatly. The turn-over seen at low energy is due to the finite analysis threshold. Even at high energy the resolution is poor - there is little difference in the shape between CC and the NC signal. The 'blinkers' used here have the same shape as the optimized reflectors used in [2] with a cutoff angle of 56 degrees so that the PMTs see direct light out to this angle. However the area of the PMT illuminated at these large angles is small and goes to zero at the cutoff angle. Consequently, there is *no* fallback option with reflectors. To use reflectors we *must* be confident they will work.

References

[1] SNO-STR-88-126

[2] SNO-STR-90-27

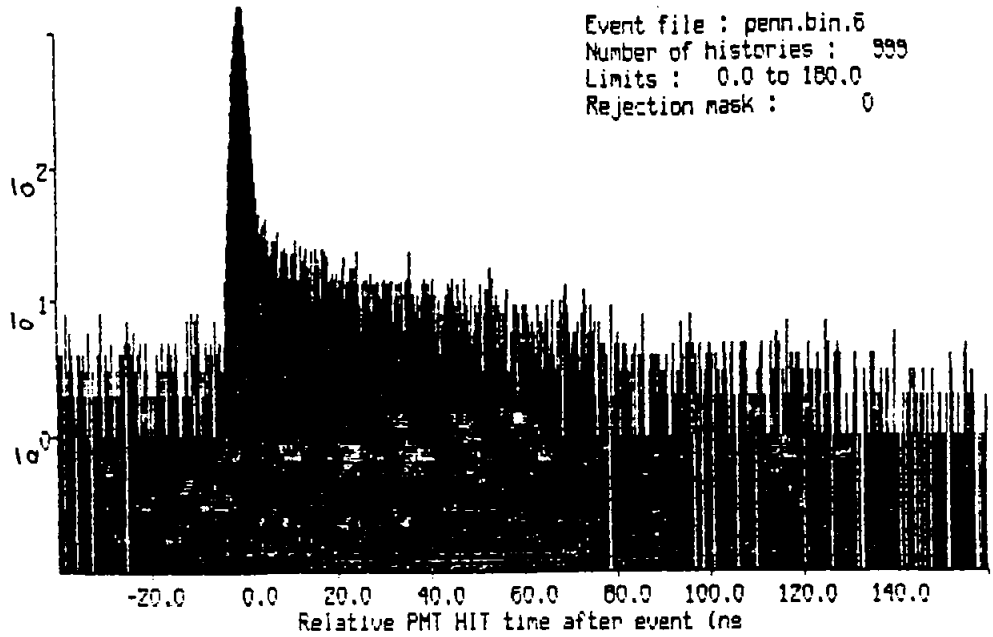
Event file : penn.bin.6
Number of histories : 999
Limits : 0.0 to 180.0
Rejection mask : 0
10^2
10^1
10^0
-20.0 0.0 20.0 40.0 60.0 80.0 100.0 120.0 140.0
Relative PMT HIT time after event (ns

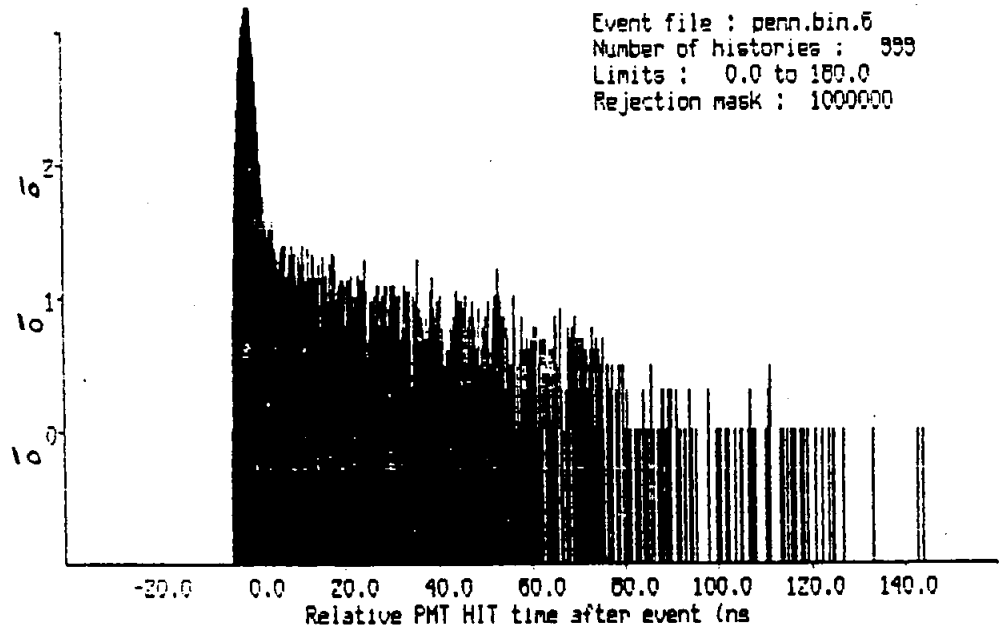
Event file : penn.bin.6
Number of histories : 999
Limits : 0.0 to 180.0
Rejection mask : 1000000
10^2
10^1
10^0
-20.0 0.0 20.0 40.0 60.0 80.0 100.0 120.0 140.0
Relative PMT HIT time after event (ns

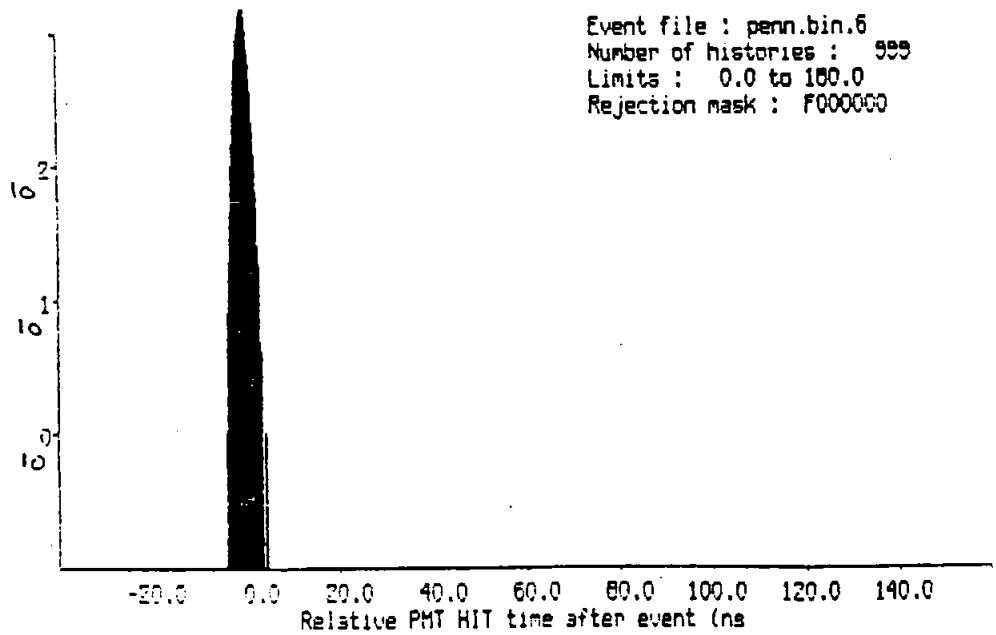
Event file : penn.bin.6
Number of histories : 999
Limits : 0.0 to 180.0
Rejection mask : F000000
10^2
10^1
10^0
-20.0 0.0 20.0 40.0 60.0 80.0 100.0 120.0 140.0
Relative PMT HIT time after event (ns

Fig 1

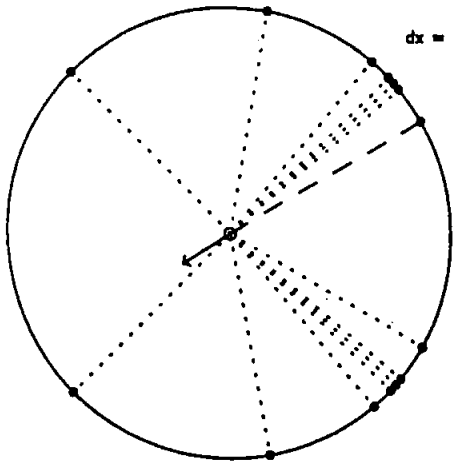
dx = −4.9 dy = −3.1 dt = 0.044

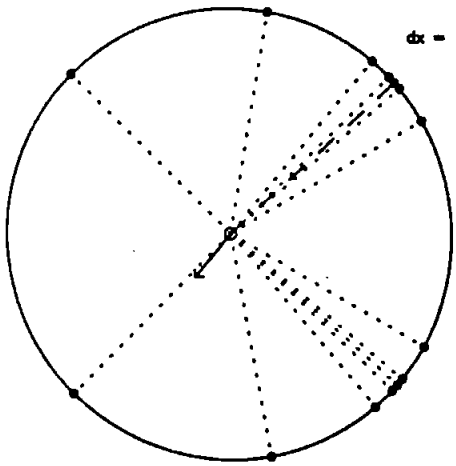
dx = −3.4 dy = −4.1 dt = 0.073

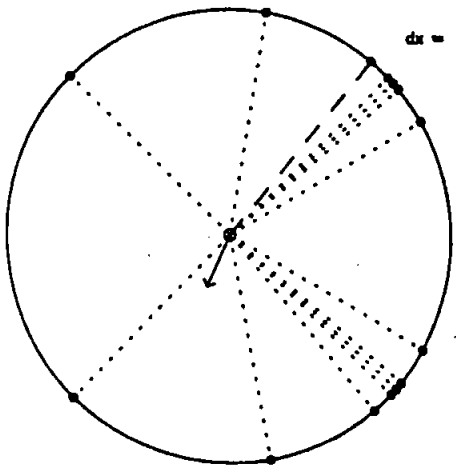
dx = −2.2 dy = −4.7 dt = 0.098

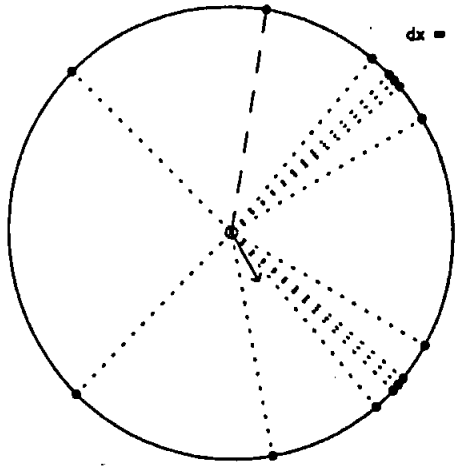

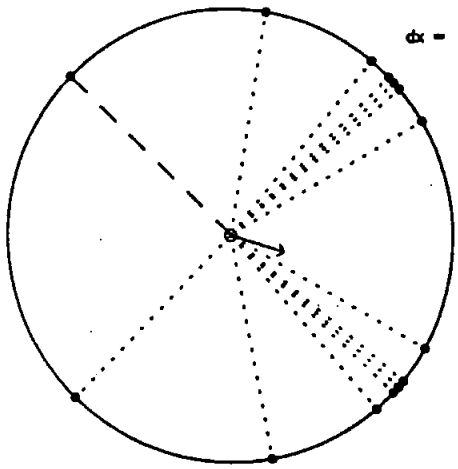

Fig 2

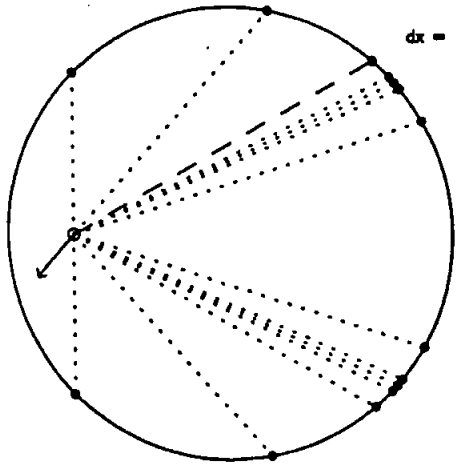
dx = −4.0 dy = −4.6 dt = 0.010

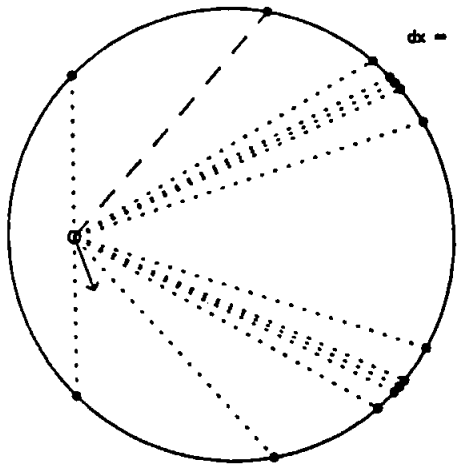
dx = 2.5 dy = −6.9 dt = 0.226

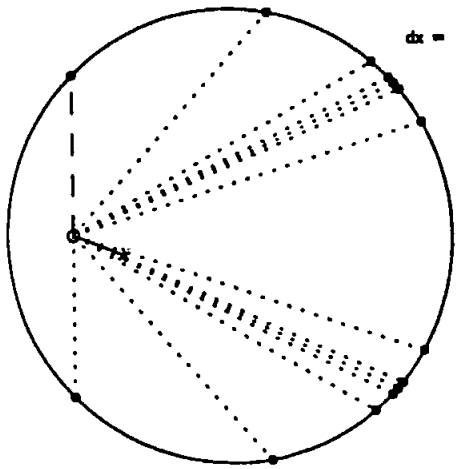
dx = 23.9 dy = −9.3 dt = 0.934

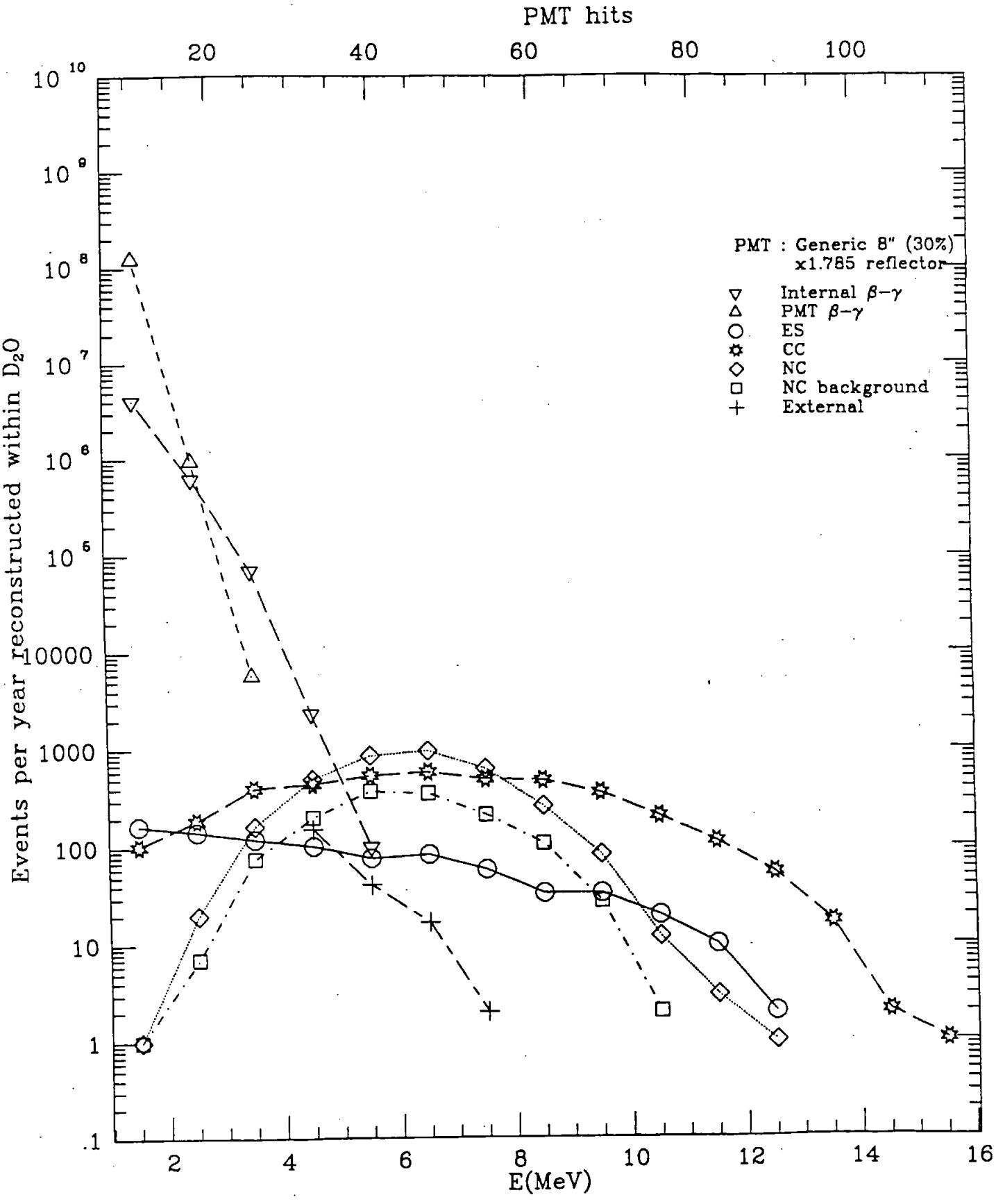
PMT hits
20
40
60
80
100
Events per year reconstructed within D_2O
10^{10}
10^{9}
10^{8}
10^{7}
10^{6}
10^{5}
10000
1000
100
10
1
.1
PMT : Generic 8" (30%)
x1.785 reflector
Internal $\beta-\gamma$
PMT $\beta-\gamma$
ES
CC
NC
NC background
External
2
4
6
8
10
12
14
16
E(MeV)

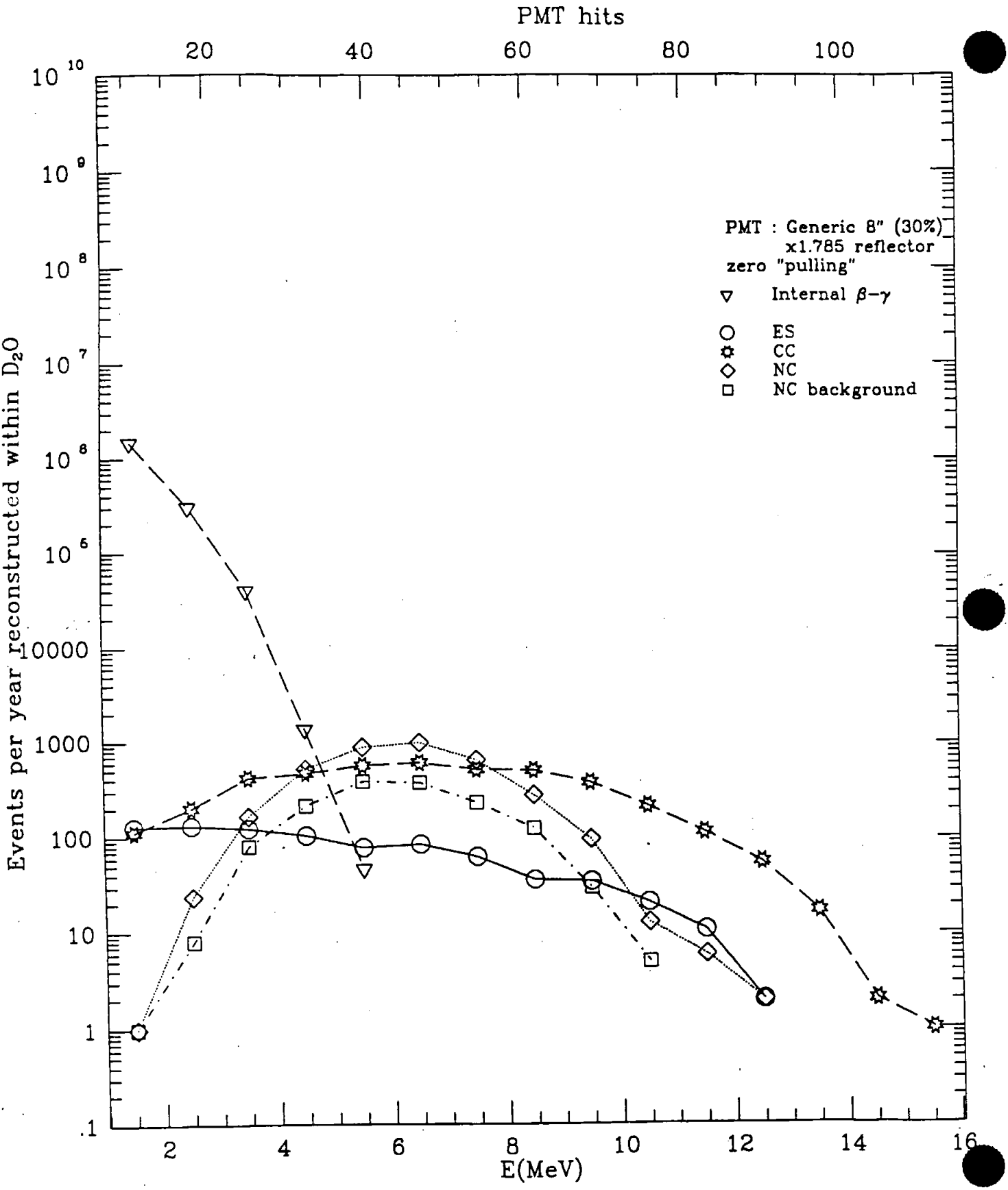
PMT hits
20
40
60
80
100
10^{10}
10^{9}
10^{8}
10^{7}
10^{6}
10^{5}
10000
1000
100
10
1
.1
Events per year reconstructed within D_2O
PMT : Generic 8" (30%)
x1.785 reflector
zero "pulling"
Internal $\beta-\gamma$
ES
CC
NC
NC background
2
4
6
8
10
12
14
16
E(MeV)

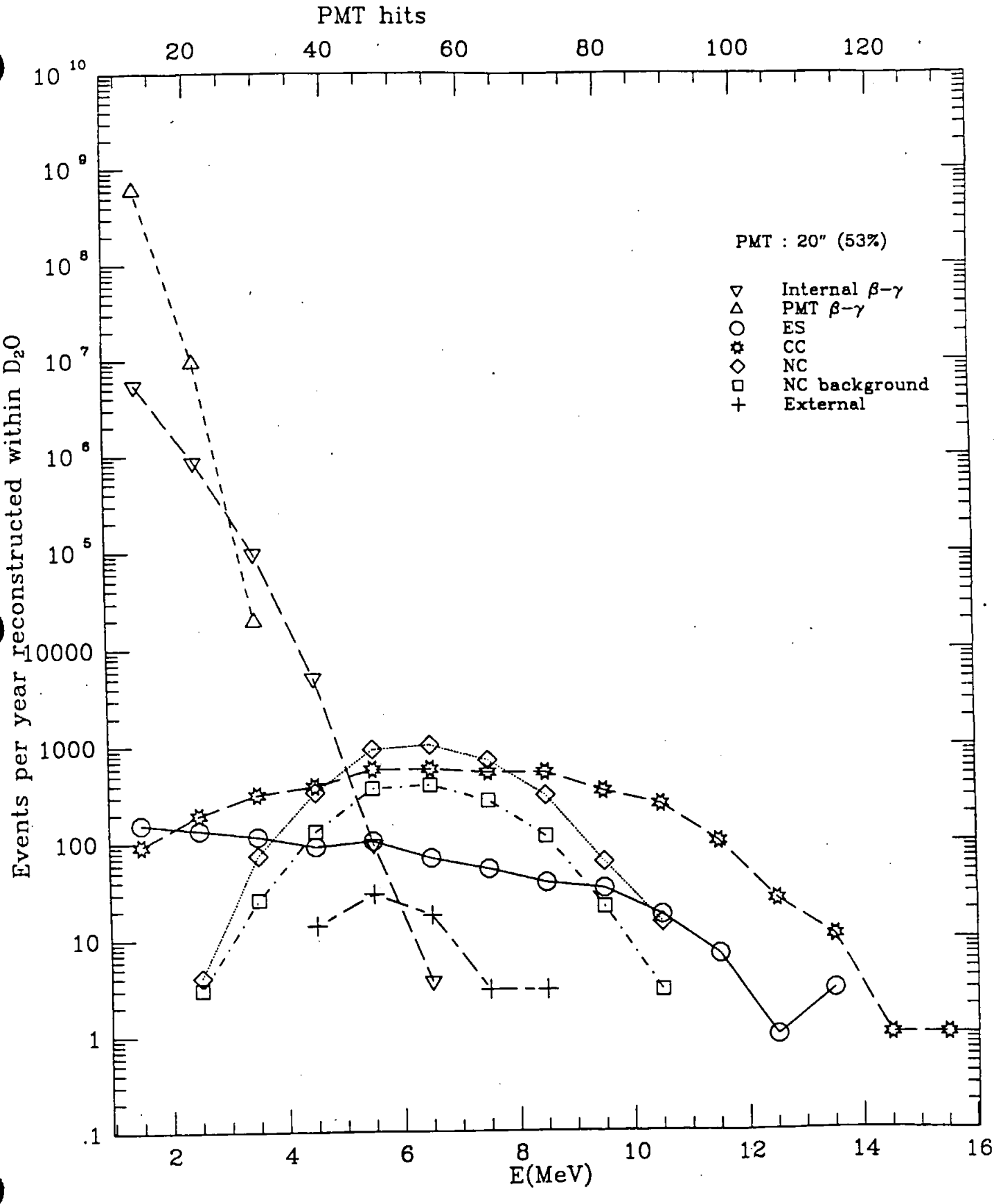
PMT hits
20
40
60
80
100
120
10^{10}
10^{9}
10^{8}
10^{7}
10^{6}
10^{5}
10000
1000
100
10
1
.1
Events per year reconstructed within D_2O
PMT : 20" (53%)
Internal $\beta-\gamma$
PMT $\beta-\gamma$
ES
CC
NC
NC background
External
2
4
6
8
10
12
14
16
E(MeV)

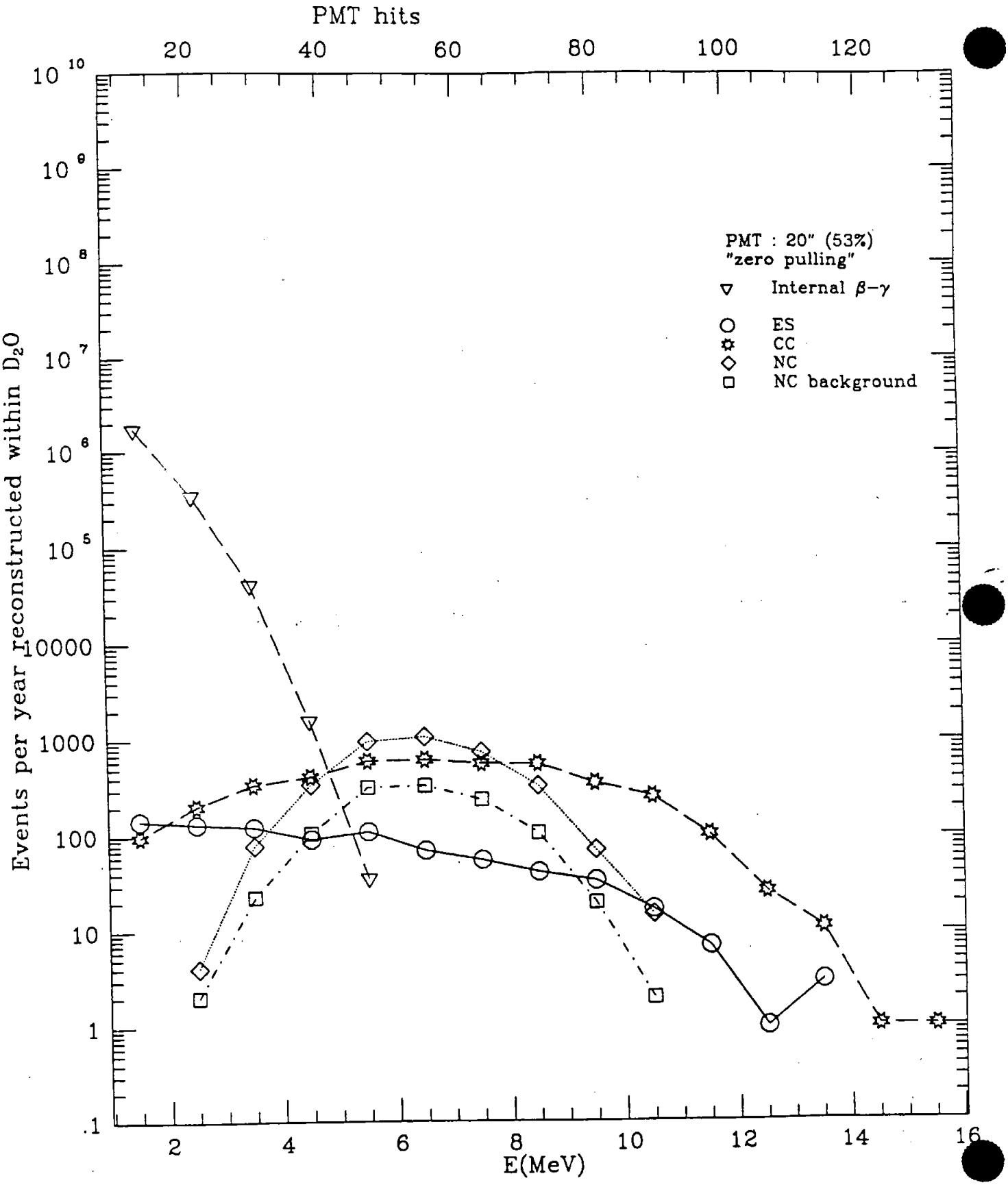
PMT hits
20
40
60
80
100
120
10^{10}
10^{9}
10^{8}
10^{7}
10^{6}
10^{5}
10000
1000
100
10
1
.1
Events per year reconstructed within D_2O
PMT : 20" (53%)
"zero pulling"
Internal $\beta-\gamma$
ES
CC
NC
NC background
2
4
6
8
10
12
14
16
E(MeV)

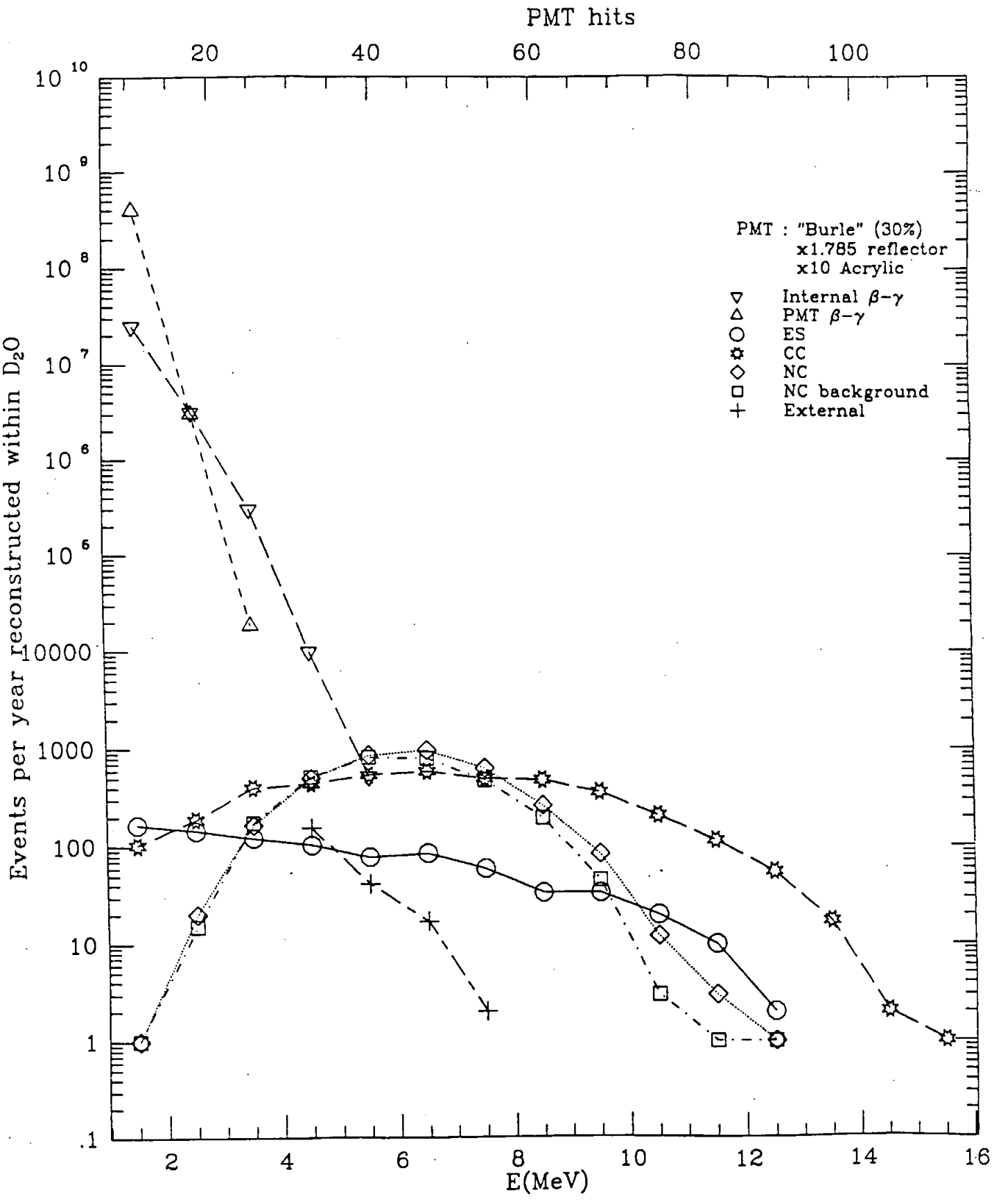
PMT hits
20
40
60
80
100
10^{10}
10^{9}
10^{8}
10^{7}
10^{6}
10^{5}
10000
1000
100
10
1
.1
Events per year reconstructed within D_2O
PMT : "Burle" (30%)
x1.785 reflector
x10 Acrylic
Internal $\beta-\gamma$
PMT $\beta-\gamma$
ES
CC
NC
NC background
External
2
4
6
8
10
12
14
16
E(MeV)

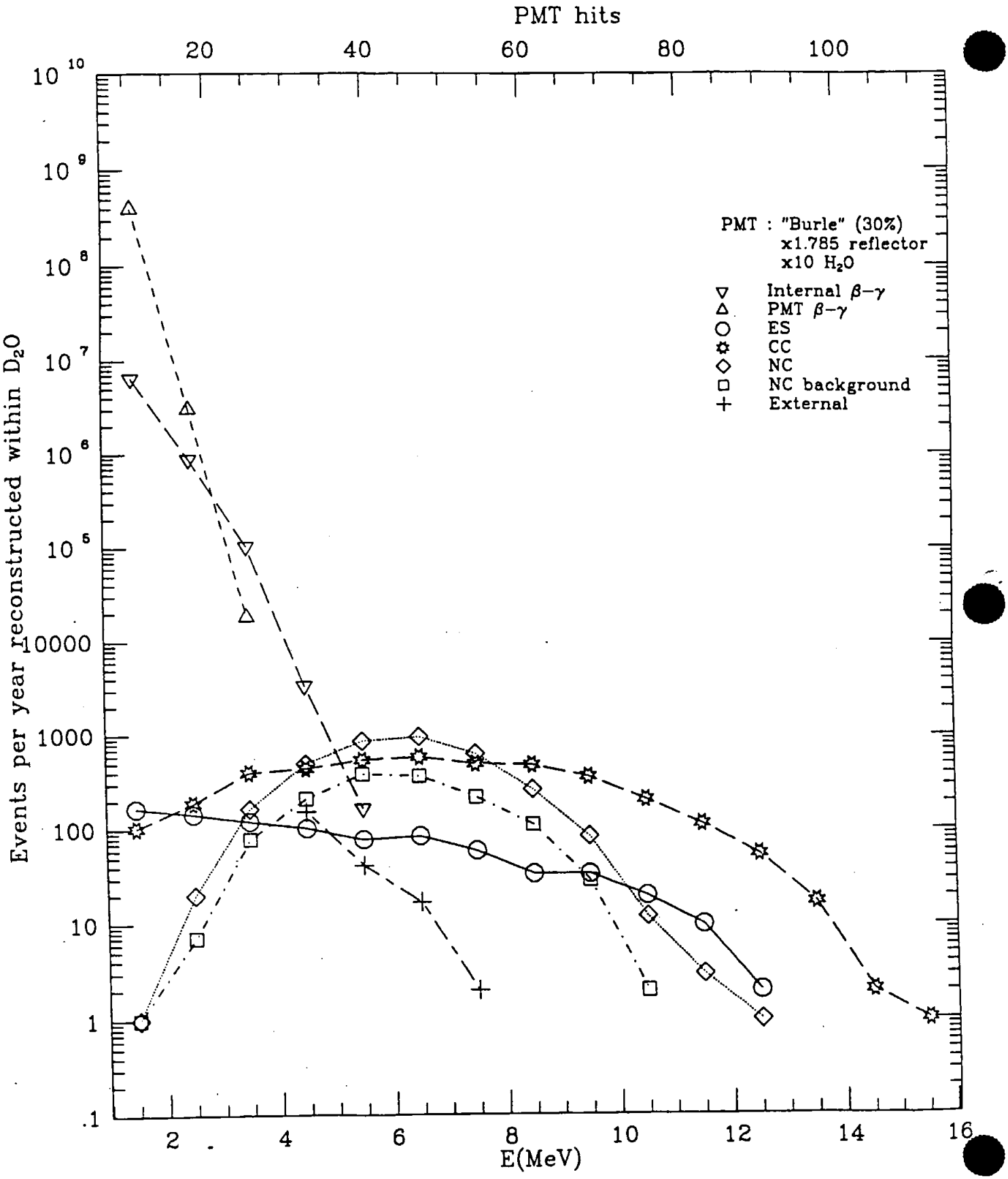
PMT hits
20
40
60
80
100
10^{10}
10^{9}
10^{8}
10^{7}
10^{6}
10^{5}
10000
1000
100
10
1
.1
Events per year reconstructed within D_2O
PMT : "Burle" (30%)
x1.785 reflector
x10 H_2O
Internal $\beta-\gamma$
PMT $\beta-\gamma$
ES
CC
NC
NC background
External
2
4
6
8
10
12
14
16
E(MeV)

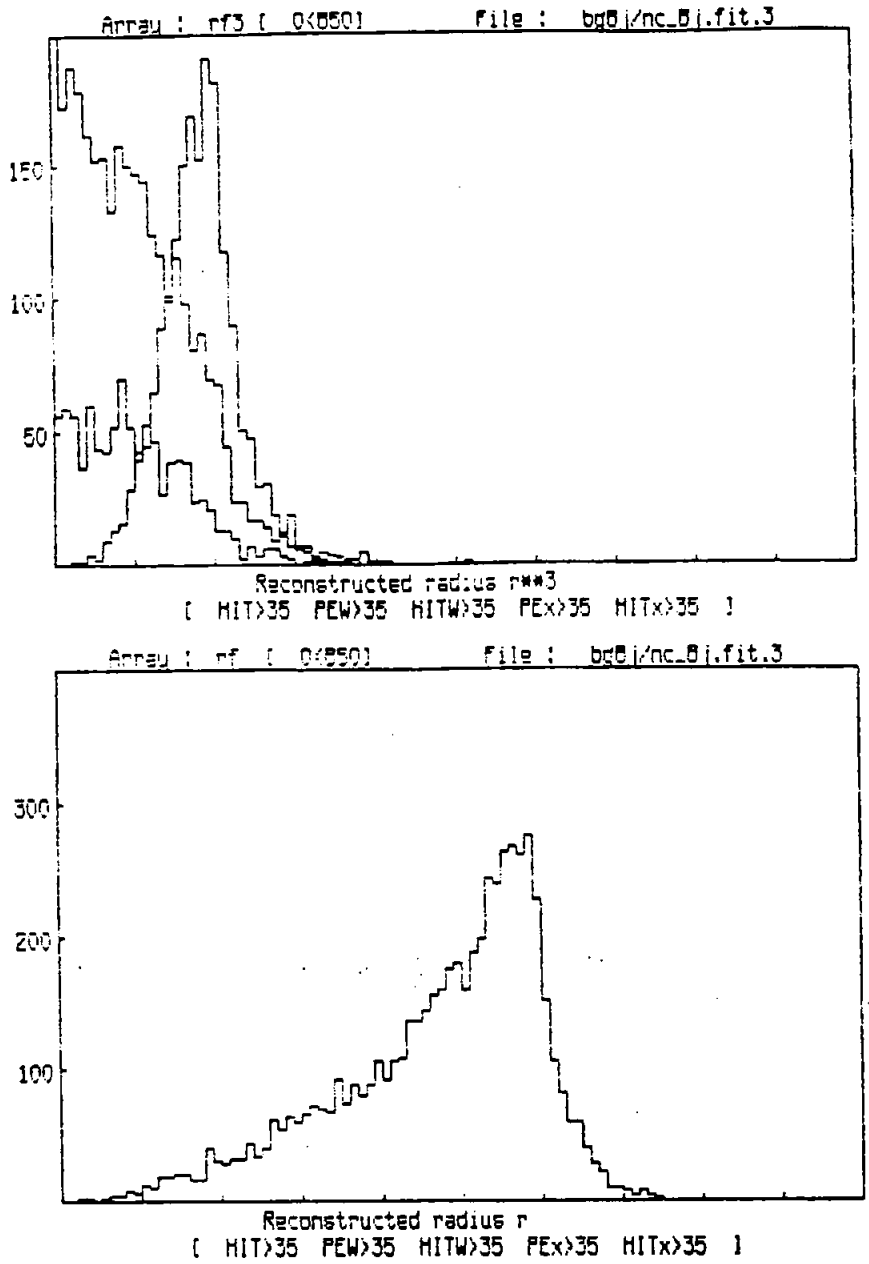

5.0 MeV

NC

x10 Acrylic

Fig 11

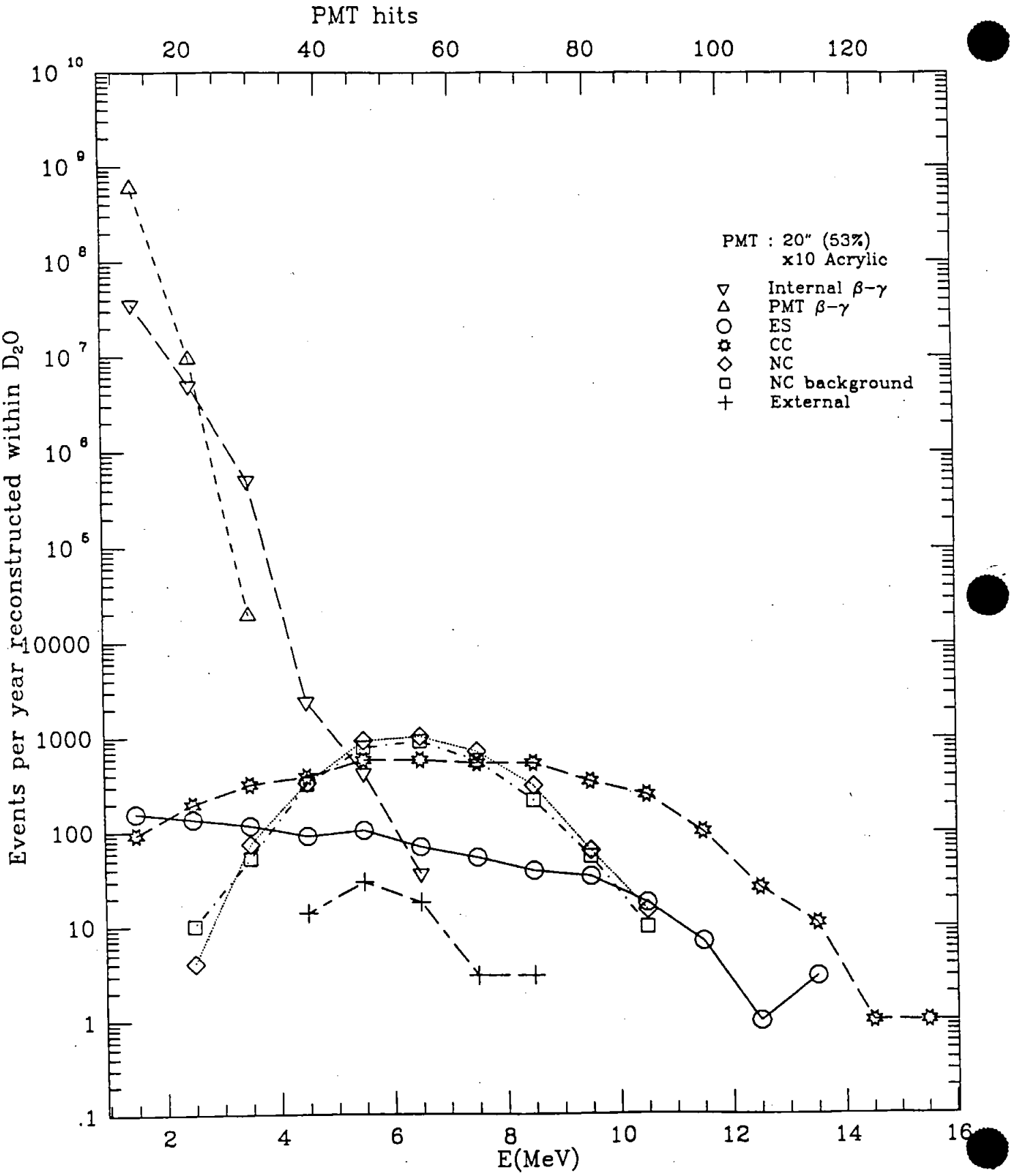
PMT hits
20
40
60
80
100
120
Events per year reconstructed within D_2O
10^{10}
10^{9}
10^{8}
10^{7}
10^{6}
10^{5}
10000
1000
100
10
1
.1
PMT : 20" (53%)
x10 Acrylic
Internal β−γ
PMT β−γ
ES
CC
NC
NC background
External
2
4
6
8
10
12
14
16
E(MeV)

[20 ton - x10 in]

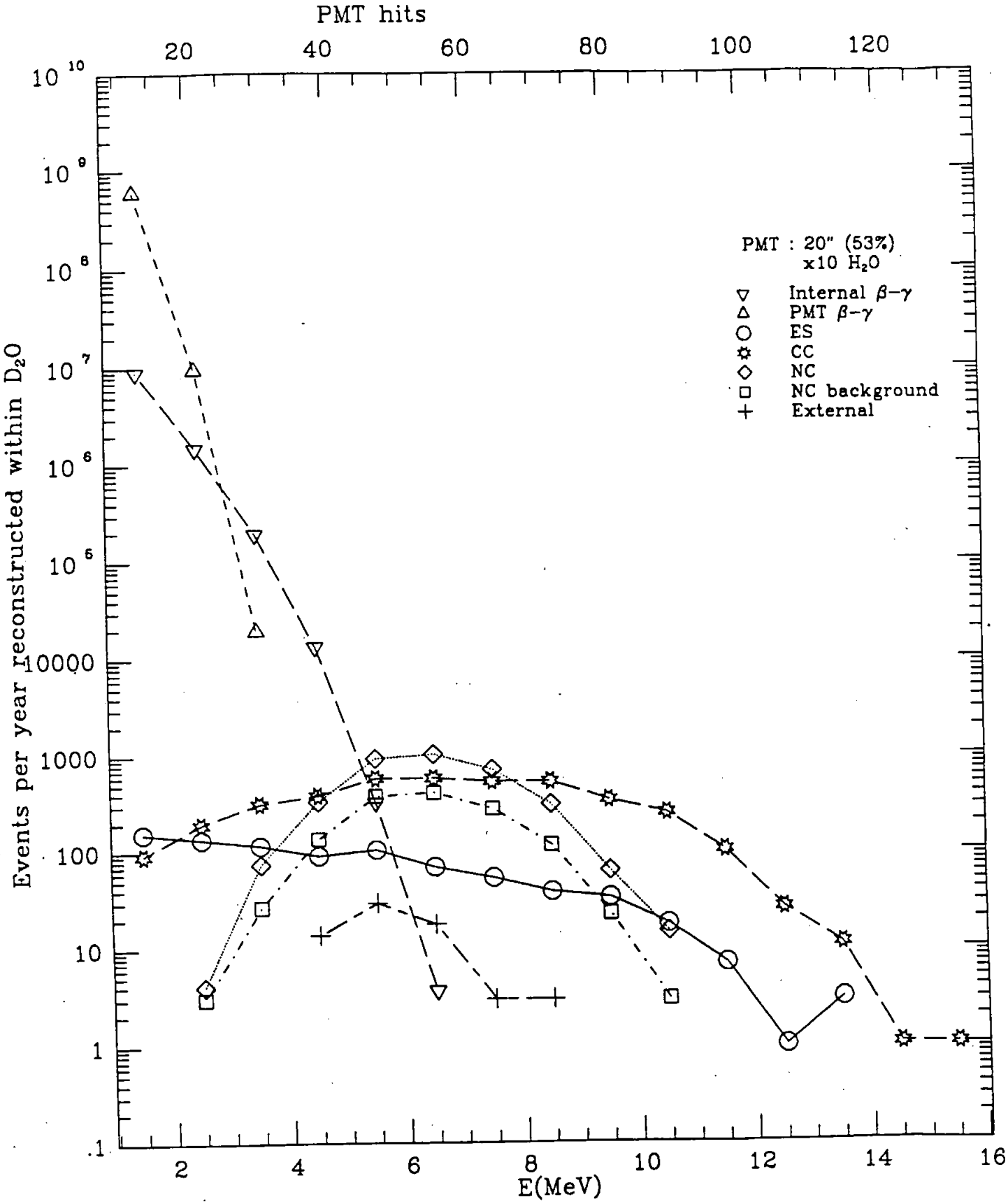

Fig 12

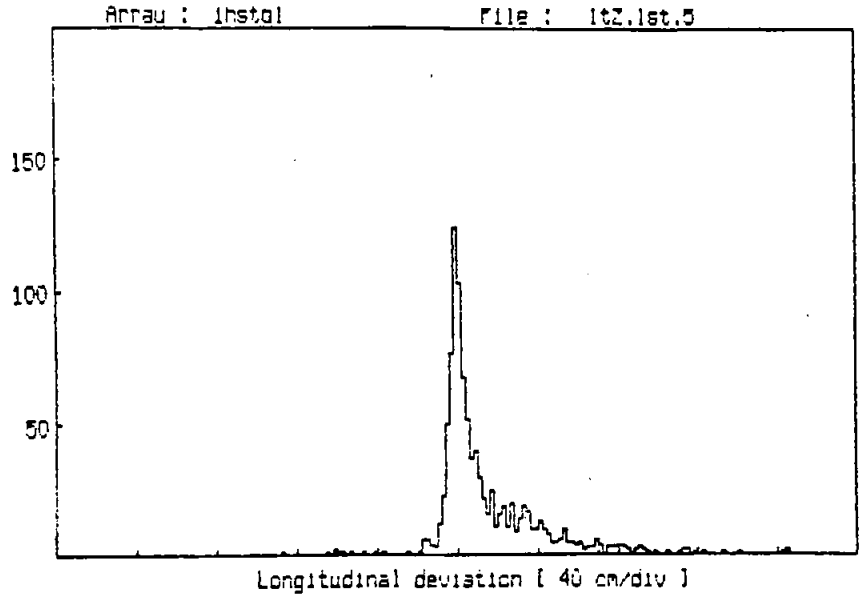
Array : ihstgl
File : lt2.lst.5
150
100
50
Longitudinal deviation [40 cm/div]

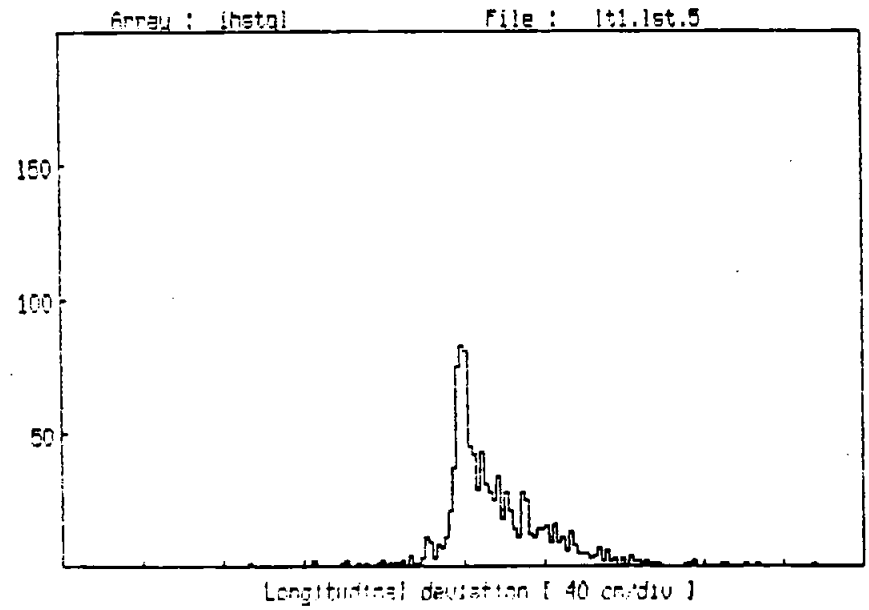
Array : ihstgl
File : lt1.lst.5
150
100
50
Longitudinal deviation [40 cm/div]

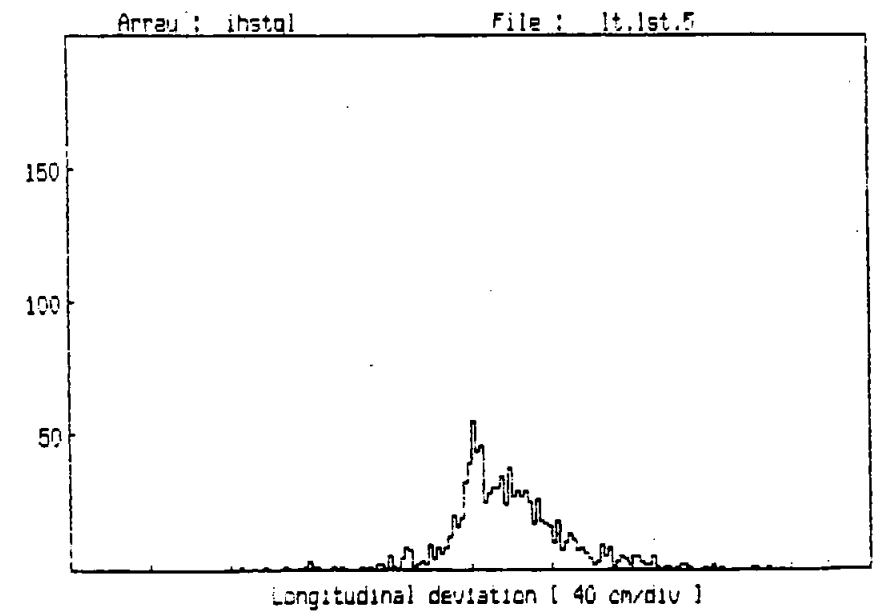
Array : ihstgl
File : lt.lst.5
150
100
50
Longitudinal deviation [40 cm/div]

Fig 14

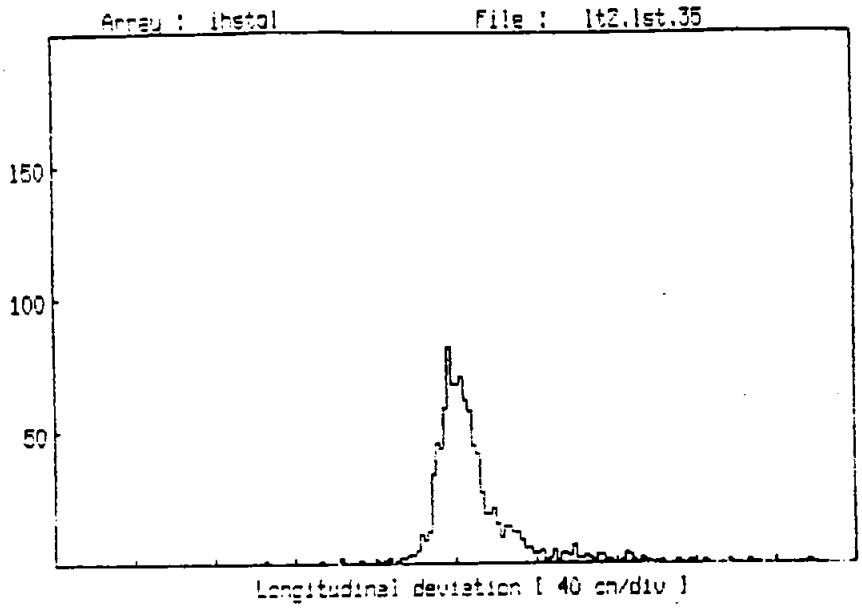
Array : ihstol
File : lt2.lst.35
150
100
50
Longitudinal deviation [40 cm/div]

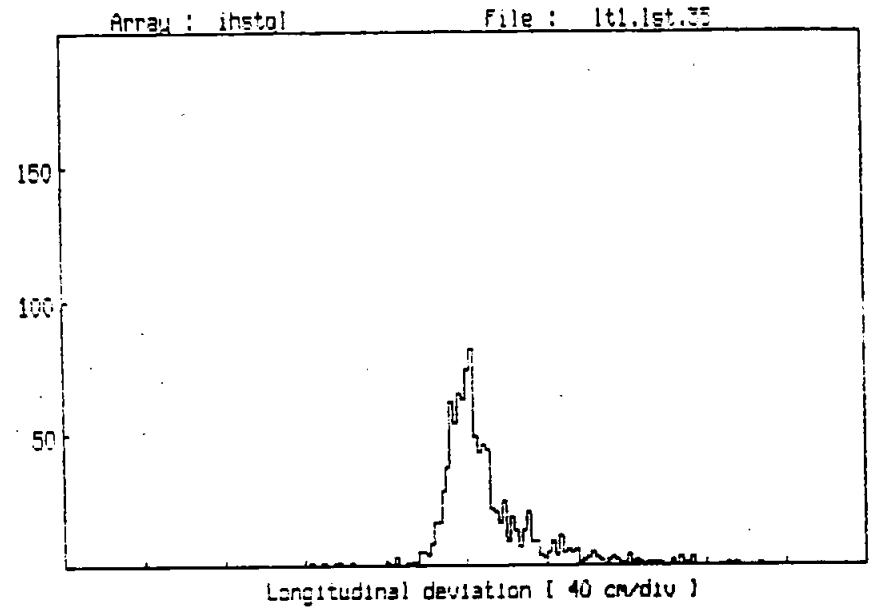
Array : ihstol
File : lt1.lst.35
150
100
50
Longitudinal deviation [40 cm/div]

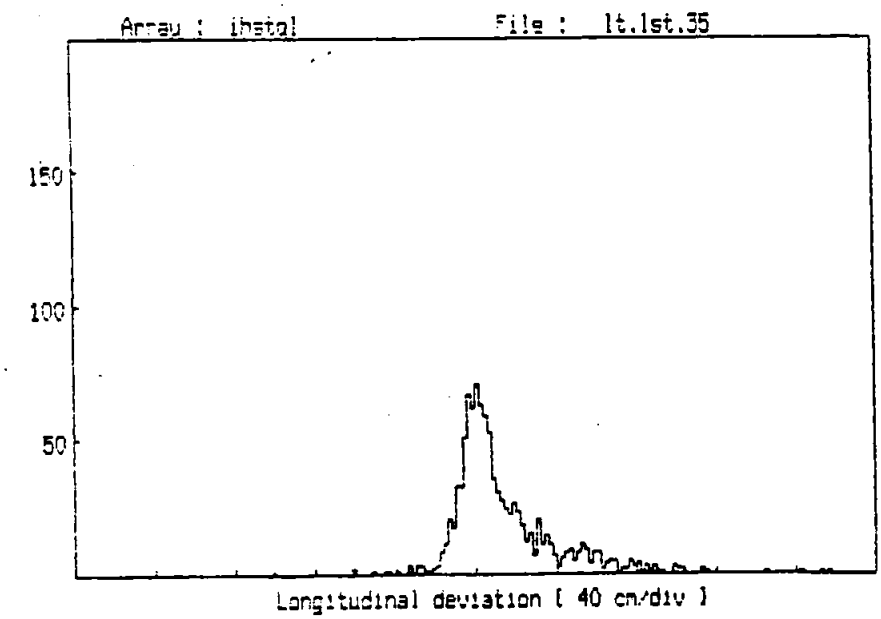
Array : ihstol
File : lt.lst.35
150
100
50
Longitudinal deviation [40 cm/div]

Fig 15

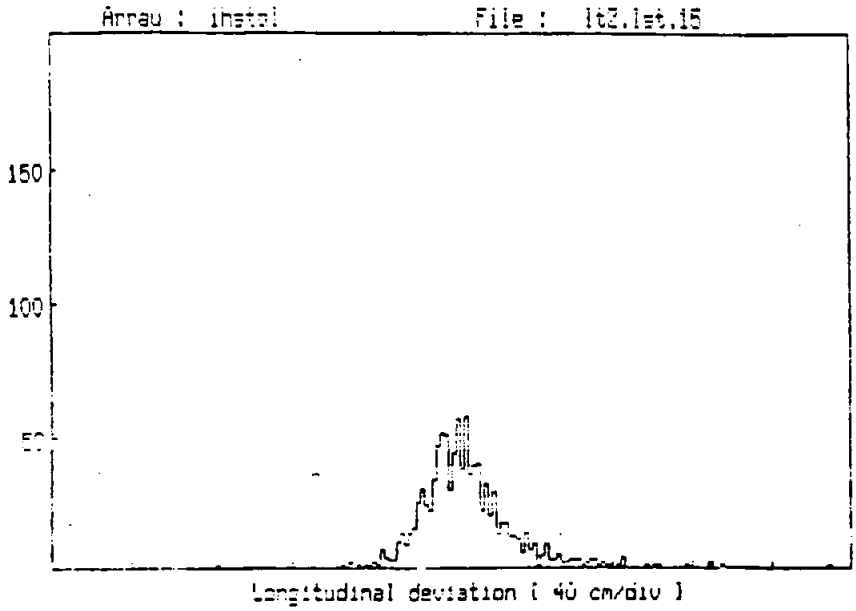
Array : ihsto!
File : lt3.lst.15
150
100
50
Longitudinal deviation [40 cm/div]

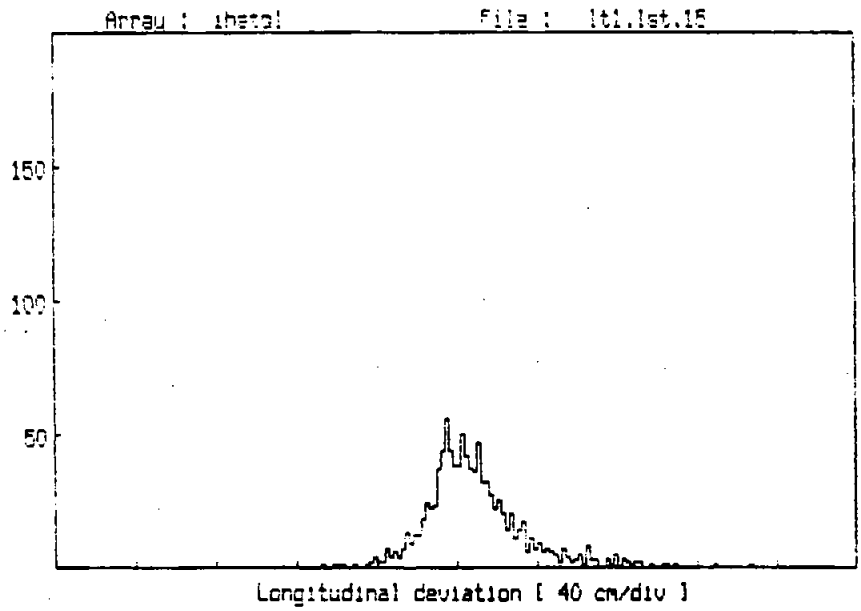
Array : ihsto!
File : lt1.lst.15
150
100
50
Longitudinal deviation [40 cm/div]

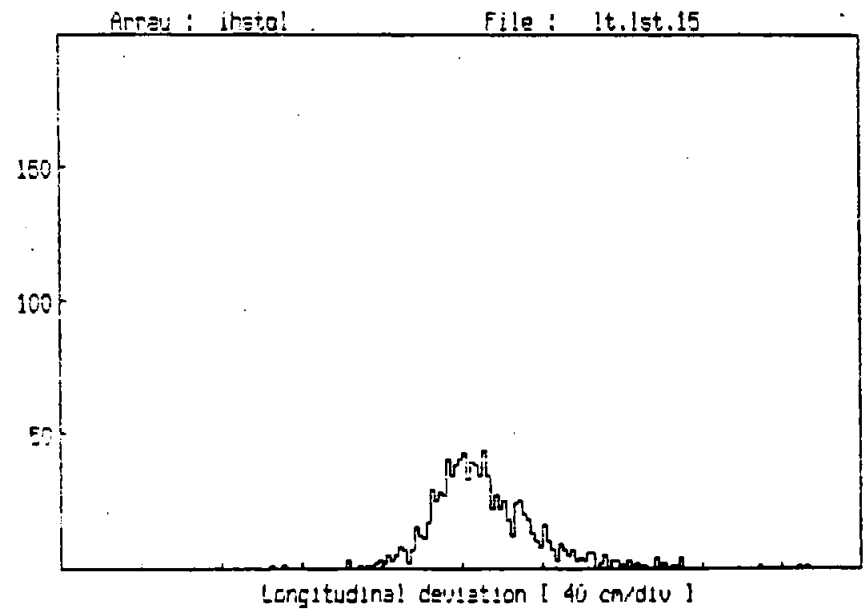
Array : ihsto!
File : lt.lst.15
150
100
50
Longitudinal deviation [40 cm/div]

Fig 16